Evaluation Using Digital Image Correlation and Finite Element method of Stress Intensity Factors and T-stress

M.L.Hattali*, H. Auradou, M. François, V. Lazarus

Laboratoire FAST, Université Paris-Sud, Université Pierre et Marie Curie–Paris 6, CNRS, Bat. 502, Campus Univ., Orsay, F-91405, France
* Corresponding author: hattali.lamine@gmail.com

Abstract A controlled crack growth in PMMA was achieved in Wedge-Splitting Test (WST) by regulating the cross-head speed of loading by a computer-driving testing device. The fracture behavior of a crack propagating was investigated quantitatively by both numerical modeling and experiment using Finite Element Method (FEM) and Digital Image Correlation (DIC). A two-parameter fracture mechanics approach, describing the near-crack-tip stress field, was applied to determine the stress intensity factor (SIF) and the coefficient of higher order term (T-stress). In both methods, it was shown that the stress intensity factor versus crack length remains constant whereas the T-stress varies from negative to positive. This later variation is similar to the three point bend beam, but different from the compact tension specimen, for which the T-term is always positive. Using Digital Image Correlation (DIC), the stress intensity factor and T stress were estimated with 10% and 15% uncertainty in a complex loading set-up without having to do a numerical modeling of the experiment.
Keywords Crack path propagation, Digital Image Correlation, Finite Element Method, Stress intensity factor, T-stress

1. Introduction

Fracture propagation in brittle or quasi brittle material is dominated mainly by the near-tip stress field. The stress intensity factors "K" gives the magnitude of the stress field ahead of a crack tip and fracture propagates when a critical stress intensity factor is reached. There are experimental evidences that the stress contributions acting at largest distance from the crack tip may affect fracture mechanics properties [1]. The constant stress contribution (first "higher-order" term of the Williams stress expansion, denoted as the T-stress term) is the next important parameter. It is well known that for crack growth under mode I loading (i.e., $K_{II} = 0$) the straight crack path is stable when $T < 0$ and unstable for $T > 0$ [2]. In the brittle or quasi-brittle materials, the determination of a two-parameter fracture mechanics "K" and T-stress as function of crack length or crack velocity is often difficult. To measure the stress field during the fracture propagation, we need to perform stable fracture tests beyond the maximum load. This is not an easy task! Sophistical and expensive test stability control apparatus (i.e. closed loop control unit with e.g. crack tip opening displacement as a feedback signal) may be used to perform such tests. . However, these systems are often not available inlaboratories.
The wedge-splitting test (WST), first used by Linsbauer and Tscheg [3] and later developed by Brühwiler and Wittmann [3], is a test that permits to propagate stable cracks. . The WST has been extensively used for experimental (e.g. [5-6]), numerical (e.g. [7-8]) and inverse analysis studies (e.g. [9]). In spite of its advantages, the fracture parameters for the WST are not widely reported. The purpose of this paper is to study, using both numerical and experimental approaches, the variation of stress intensity factor or T-stress as function of crack path position. Digital Image Correlation (DIC) is used to follow the crack propagation. Based on displacements evaluation, crack tip position, Stress intensity factor "K" and T-stress are determined. Secondly, we performed by means of a constraint-based two-parameter fracture mechanics approach, a numerical analysis of near-crack-tip stress field using the Finite Element Method (Abaqus 6.6 software) [10]. In the numerical approach, the wedge

displacement load versus crack tip position data was used as boundary load conditions to calculate both stress intensity factor "K" and T-stress. Their values are compared with the result obtained by the Digital Image Correlation (Q4-DIC software) [11]. Finally, the performances of the two global approaches are compared.

2. Experimental configuration

The experimental setup is shown in Figure 1a and b. A vertical load is applied by means of a metallic wedge at the mouth of the notched sample. The sample is supported along its basis. To minimize friction between wedge and lateral supports, two lines of rollers are used. During testing, the wedge pierces the sample and the crack generated at the tip of the notch propagates in stable way. The crack grows until it reaches the bottom of the sample, splitting it into halves.

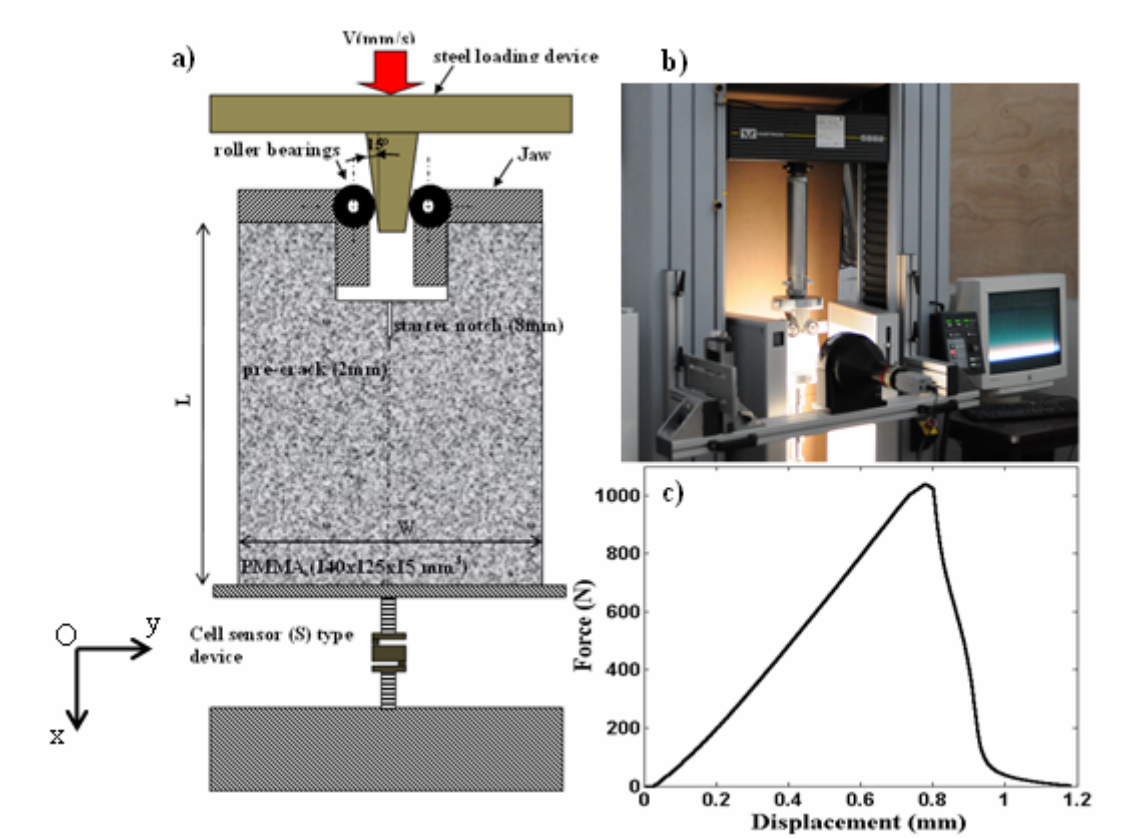

Figure 1. a) Experimental set-up of the Wedge Splitting loading. b) A telecentric lens is used to minimize artifacts induced by out-of-plane motions. c) Typical load- wedge displacement curve from PMMA fracture test.

Due to the compressive stresses in front of the crack tip and due to the small amount of elastic energy stored in the specimen, the crack propagates with a velocity proportional to V_{wedge}. The elastic energy stored in the testing device is much lower compared to other common test methods because the wedge angle (here choose to 15°) enhances the effect of the vertical force applied by the machine. The material used is Polymethyl methacrylate (PMMA) from Altuglas International (Perspex sheets). This material is brittle with a Young's modulus E= 2800 MPa and Poisson's ratio ν=0.33. The specimen is prepared from rectangular plates of length L=140mm, width W=125mm, and thickness H=15mm. A notch is machined i) by cutting out a 25x25x15mm^3 parallelepipeds from the middle of one of the WxH edges; ii) by subsequently adding a 8 mm long 800 µm thick groove with a diamond saw; and

iii) by finally introducing a seed crack (~2mm-long) with a razor blade. The test is conducted at room temperature (20 °C), under displacement control at 1 μm/s using a testing machine of 1 kN capacity (Instron 5882). The specimens exhibited a linear load–displacement diagram prior to fracture, confirming the predominantly linear elastic behavior of the material (Figure 1c). During the test, the surface of the sample is observed, with a CCD camera, (pixeLINK®, definition: 2500 x 1600 pixels, digitization: 8 bits) operating at 0.1 Hz and equipped with a telecentric objectif (GO Edmund, Techspec® gold series, Max distorsion: 0.35%, telecentricity: < 0.2°). The telecentric is used to minimize artifacts related to out-of-plane motions. The physical pixel size corresponds to 44.2 μm. Prior to the experiment, surface of the sample is painted in white and speckled with black paint. Two halogen lights are used for illuminating. For a realistic simulation, we need to obtain the typical wedge displacement-crack length curve from mechanical test and the crack path trajectory. These informations are directly measured from the location of crack tip via the camera using Digital Image Correlation (Figure 2a and b).

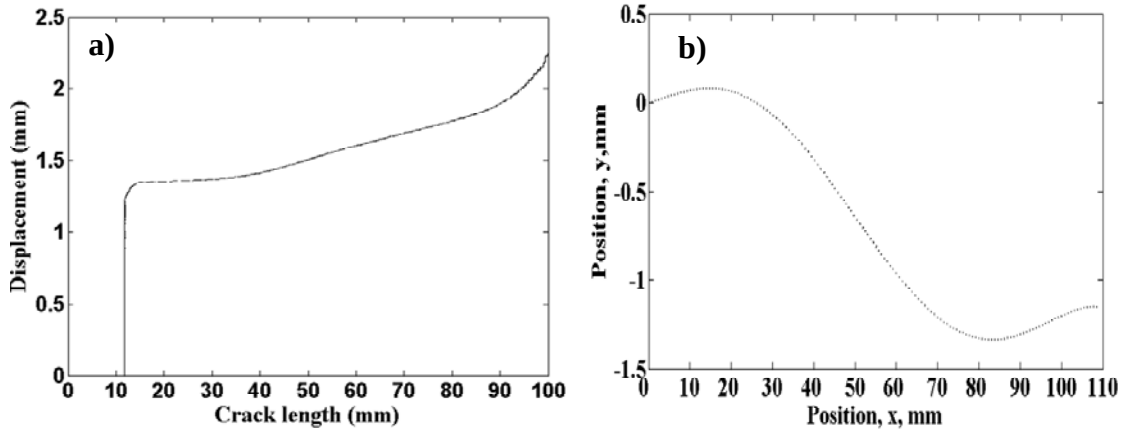

Figure 2. a) Displacement-crack length curve from PMMA fracture test, b) Crack path trajectory determined by DIC.

3. Finite element analysis (Abaqus)

Two-dimensional linear elastic fracture mechanics is retained to model the Wedge Splitting Test (WST) using a finite element method (Abaqus 6.6 software). To be in agreement with the experimental conditions, the choice of plane-stress state conditions was assumed. The computation of the stress intensity factor (K) and T-stress based on the domain integral "J" is carried out using six contours [10,12]. Apart from the first contour, the J-integral is path independent for the remaining 5 contours surrounding the crack tip. The material model was linear elastic, with the same properties for the experimental tests. The loading wedge is modeled as rigid bodies. The specimen is loaded by applying a displacement to the wedge in the vertical direction using an experimental displacement versus crack length data in the loading boundary conditions and taking under consideration the crack path trajectory (see Figure 2a and b. All other motions of the wedge are restrained. Surface-to-surface contact with a finite-sliding formulation is defined between the wedge and the rolling specimens, on the one side, and the specimen and the support, on the other. We assume that the contact is frictionless. Two analysis steps are used. In the first step, contact is established between the wedge and the rolling specimen by applying a small displacement (1×10^{-3} mm) in the vertical direction. In the second step controlled displacement loading of the wedge is applied. The virtual crack extension direction is specified with the q-vector. In the present model, it is defined with the starting point at the crack tip and the end point at the red dot, as shown in Figure 3.

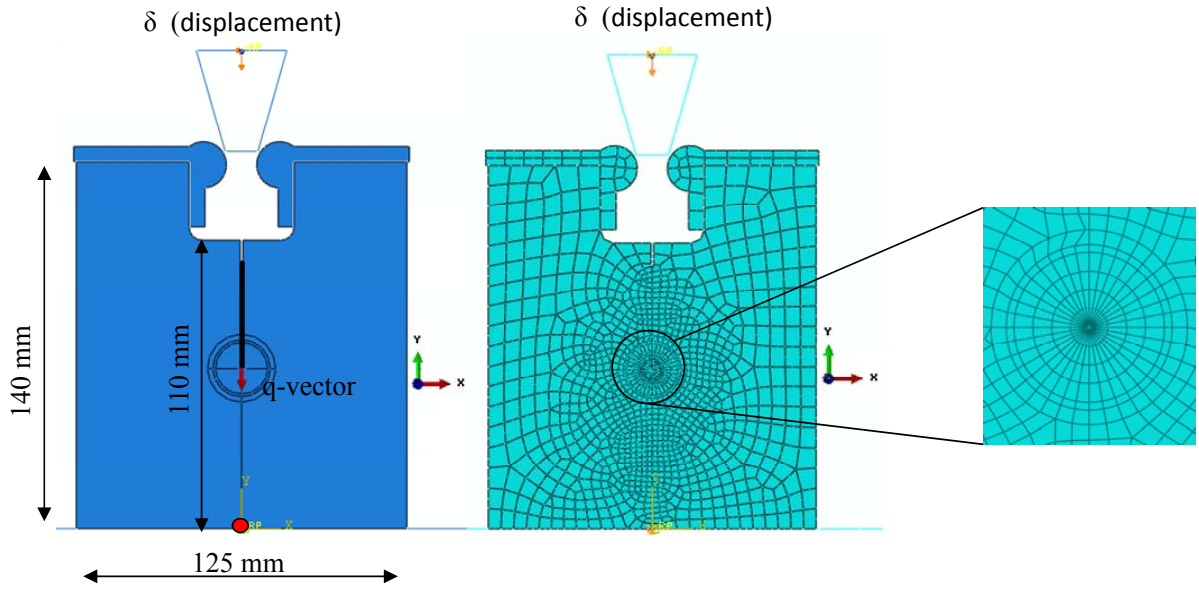

Figure 3. Partitioned two-dimensional Wedge Splitting Test and mesh strategy adopted around crack-tip.

For a sharp crack, the strain field becomes singular at the crack tip. Including the singularity at the crack tip for a small-strain analysis improves the accuracy of strain calculations, the J-integral and stress intensity factors. The partitioning of the geometry is defined by the circular lines centered on the crack tip (Figure 3); this partitioning strategy facilitates the generation of a focused mesh. The remaining portion of the model is free meshed using the "medial axis" meshing algorithm. The crack tip is meshed using a ring of collapsed 8-node bilinear, reduced integration (CPS8R) elements. To obtain a $1/\sqrt{r}$ singularity term, the following conditions must be met:

1. The elements around the crack tip must be focused on the crack tip. One edge of each element must be collapsed to zero length so that the nodes of this zero length edge are located at the crack tip.
2. The "midside" nodes of the edges radiating out from the crack tip of each of the elements attached to the crack tip must be placed at one-quarter of the distance from the crack tip to the other node of the edge.

4. Digital Image Correlation Analysis (Q4-DIC)

Digital image correlation is a technique that allows one to retrieve displacement fields separating two digital images of the same sample at different stages of loading.
We summarize the main points here, for more information the reader shall refer for instance to [11, 15]. Generally, it is not possible to find the correspondence of a single pixel in an image in the deformed state to the image in the reference state. This is because there is not a unique correspondence. The subsets which are comprised of finite number of pixels are utilized to locate the same material point between deformed and reference states. To correlate the deformed image $\boldsymbol{g}$ to the undeformed reference image $\boldsymbol{f}$, each image is divided into small subsets and the correlation algorithm is executed from subset to subset. A digital image of a body is simply a discrete intensity record of the light levels present at various positions of the body in the smallest unit of digitization, the pixel. In an eight-bit system, light intensity at each pixel ranges in value from 0 to 255 (represented as $0 < p(x,y) < 255$). The point P(x,y) in

the reference image becomes P'(x^*,y^*) in the deformed image and Q(x,y) becomes Q'(x^*,y^*). DIC is run by comparing group of similar light intensity numbers between the two digital images to track points P and Q. Depending on the use of a first or second order approximation, 6 or 12 unknowns are available and can be found by correlation between the two images. This can be done by minimizing the global residual between the reference image f and the deformed image corrected by the displacement field g(x+u(x)) over the whole region of interest:

$$\eta^2 = \iint_\Omega \left[g(x+u(x)) - f(x)\right]^2 dx \tag{1}$$

In the following, 4-noded elements are considered (*i.e.* a Q4-DIC approach [11]). The DIC procedure applied herein consists in measuring displacement field discretized with quadratic Q4 elements. The elements size was chosen to be equal to 8 pixels. This value is a good compromise between measurement uncertainly and spatial resolution. Extracting some mechanically meaningful information using the detailed map of displacement can be performed by identifying the amplitudes of relevant reference displacement fields namely, William's series [13]. These field $\mathbf{u}=u_x+iu_y$ take the following expression in the crack frame (crack tip at the origin, and crack path along the negative x axis) resorting to the complex plane, $z=re^{i\theta}$

$$u(z) = \sum_n \left[\omega_n \Omega_n(z) + \upsilon_n \psi_n(z)\right] \tag{2}$$

With, for a mode I regime:

$$\Omega_n(z) = \frac{(-1)^{(1-n)/2}}{2\mu\sqrt{2\pi}} r^{n/2}\left[\kappa \exp\left(\frac{in\theta}{2}\right) - \frac{n}{2}\exp\left(\frac{i(4-n)\theta}{2}\right) + \left((-1)^n + \frac{n}{2}\right)\exp\left(-\frac{in\theta}{2}\right)\right] \tag{3}$$

And a mode II regime:

$$\Psi_n(z) = \frac{i(-1)^{(1-n)/2}}{2\mu\sqrt{2\pi}} r^{n/2}\left[\kappa \exp\left(\frac{in\theta}{2}\right) + \frac{n}{2}\exp\left(\frac{i(4-n)\theta}{2}\right) + \left((-1)^n - \frac{n}{2}\right)\exp\left(-\frac{in\theta}{2}\right)\right] \tag{4}$$

Where μ is Lamé's modulus, and κ is a dimensionless parameter dependent on Poisson ratio ν (*i.e.* $\kappa = \frac{3-\upsilon}{1+\upsilon}$ in plane stress, or 3-4ν in plane strain condition).

Amplitudes ω_1 and ν_1, associated with field Ω_1 and Ψ_1, are the mode I and II SIFs, K_I and K_{II}, respectively. Amplitudes ω_0 and ν_0 correspond to rigid body translations. Amplitudes ω_2 and ν_2 give access to the T-stress component, and the rigid body rotation. The crack-tip is located by canceling out amplitude ω_{-1} of the first supersingular field.

5. Results and discussion

Experimental results were obtained from the displacement fields obtained with a mesh size of 8 pixels (1 pixel→44.2 μm), over a region of interest of 2500 x 350 pixels (Figure 4).

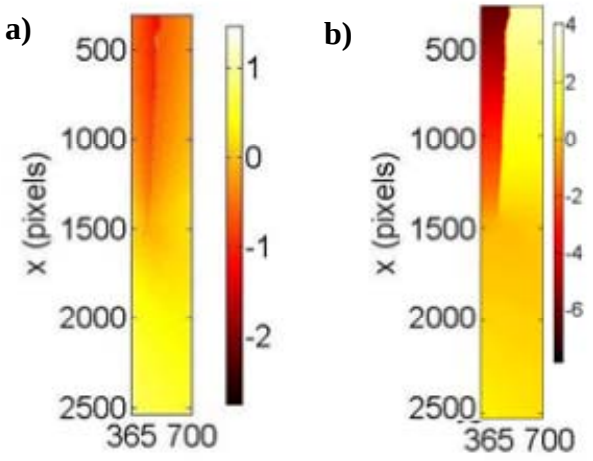

Figure 4. Horizontal (a) and vertical (b) component of the displacement field expressed in pixels as projected onto the basis of suited functions in post-processing of the measured displacement (1 pixel → 44.2 μm).

From the amplitudes ω_n and ν_n, it is possible to plot the SIF and T-stress as function of crack length. In figure 5a and 5b, the SIF obtained by DIC are shown together with the SIF obtained by Abaqus. In average the differences is 9%. For the DIC method, an error bars was estimated by extracting extreme positions of crack tip and measuring the corresponding change in K (average error bars were 11 %). For both methods, we found that K_I is constant from 40 mm to the end of sample, demonstrating that the crack propagation is stable (ie. The cracks propagates with a constant velocity), whereas K_{II} fluctuates around zero (Fig 5b). Despite an average difference of 22 %, a good agreement is found in the case of the T-stress component when compared to the FE results. This difference is compensated by error bars (an average error bar were 15%) (Fig 5c). In both case, the T-stress varies from negative value for short cracks to positive value for crack lengths above 5 mm, contrary to the compact tension geometry, where T values are always positive [14]. Compared to the stress intensity factor, the error bar in the case of T-stress is higher because the T-stress is the coefficient of higher order terms of the displacement field expansions.

Without surprise, those measures confirms Irwin's criterion $K_I=K_c$ during stable propagation and the Principle of Local Symmetry $K_{II}=0$. It confirms also Cotterell and Rice crack path stability criterion. As soon the T-stress becomes positive, the crack path doesn't remain straight (fig. 2b) and find another, not straight, path which satisfies nevertheless Irwin's criterion and the Principle of Local Symmetry. This is one more [16] experimental demonstration that this double criterion doesn't lead to a unique solution: the observed crack path is not the trivial straight one but another more stable bifurcated one.

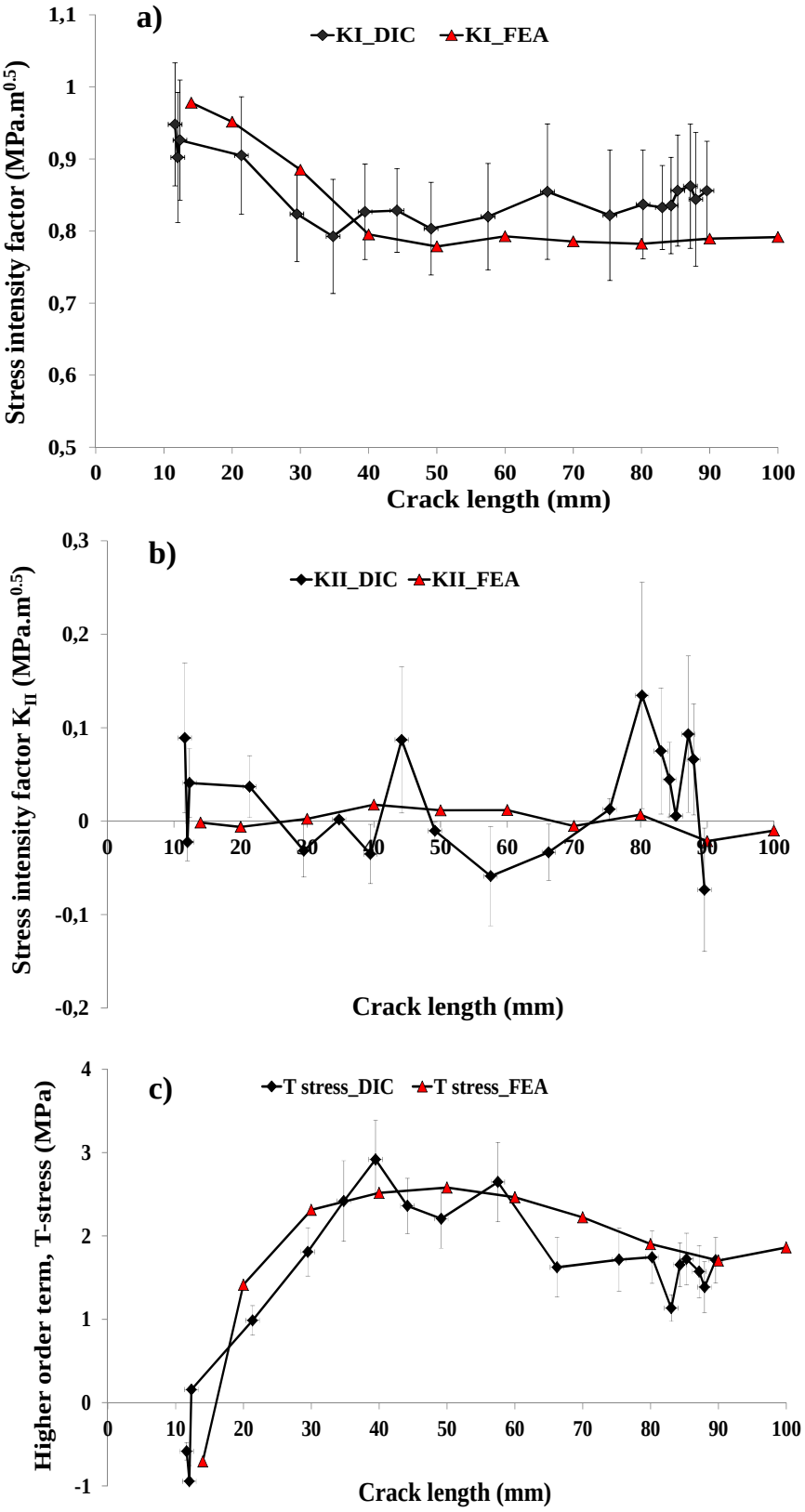

Figure 5. Comparison of (a)-(b) stress intensity factor, (c) T-stress determining using Finite Element Analysis and Digital Image correlation.

6. Conclusions

The Finite element Analysis and Direct measurement of the crack tip displacement field is performed using Abaqus software and Digital Image Correlation (Q4-DIC). In Finite Element Analysis, the two parameter fracture mechanics approach, describing the near–crack-tip stress field (SIF and T-stress) were calculated using the domain integral "J". In Digital Image Correlation, these parameters were obtained by adjusting the first supersingular term of William's series. One the crack tip was determined, the crack growth increment is estimated in addition to other global parameters such as the stress intensity factor range and T-stress. In both method, good agreement is shown and finite element analysis can be validated. The stress intensity factor versus crack length remains constant whereas the T-stress varies from negative to positive. This later variation is similar to the three point bend beam, but different from the compact tension specimen, for which the T-term is always positive. Using Digital Image Correlation (DIC), the stress intensity factor and T stress were estimated with 10% and 15% uncertainty in a complex loading set-up without the need for a numerical modeling of the experiment. The displacement and crack extension at the onset of crack propagation is important. It is expected that any model that can match all the experimentally observed features of the test will provide a significant enhancement to our present capability to predict any fracture parameter. Our wedge splitting test is particularly attractive for fundamental research and model validation because of the enhanced length of stable crack propagation. This advantage allows us the identification of crack propagation parameters during all propagation from one single test.

Acknowledgement

The authors acknowledge support of the ANR Program SYSCOMM grants ANR-09-SYSC-006 (France).

References

[1] T.Fett, A Green's function for T-stresses in an edge-cracked rectangular plate. Eng Frac Mech, 57(4) (1997) 365-373.
[2] B. Cotterell, J.R. Rice, Slightly curved or kinked cracks. Int J Fracture, 16(2) (1980) 155-169.
[3] H.N. Linsbauer and E.K. Tschegg, Fracture energy determination of concrete with cube-shaped specimens. Zement und Beton, 31 (1986) 38-40.
[4] E. Bmhwiler and E H. Wittmann, The wedge splitting test: A method of performing stable fracture mechanics tests. Engineering Fracture Mechanics, 35 (1990) 117-125.
[5] M. Elser, E. K. Tschegg, N. Finger, S. E. Stanzl-Tschegg, Fracture behaviour of polypropylene-fibre reinforced concrete: an experimental investigation. Compos Sci Technol, 56 (1996) 933–45.
[6] J. Scheibert, C. Guerra, F. Célarié, D. Dalmas and D. Bonamy, Brittle-Quasibrittle Transition in Dynamic Fracture: An Energetic Signature. Physical Review Letters, 104 (2010) 045501.
[7] L. Ostergaard, Early-age fracture mechanics and cracking of concrete-experiments and modelling. Ph.D. Thesis. Department of Civil Engineering, Technical University of Denmark; 2003.
[8] G.V. Guinea, M. Elices, J. Planas, Stress intensity factors for wedge-splitting geometry. Int J Fracture, 81 (1996) 113–24.

[9] N.S. Que, F. Tin-Loi, An optimization approach for indirect identification of cohesive crack properties. Comput Struct, 80(16-17) (2002) 1383-92.
[10] ABAQUS Software (2006) User's manual, version 6.6. Karlsson and Sorensen Inc, Hibbitt.
[11] S.Roux, F. Hild, Stress intensity factor measurement from digital image correlation:post-processing and integrated approaches. Int J Fract, 140 (2006) 141–157.
[12] F. Erdogan, G. C. Sih, On the crack extension in plates under plane loading and transverse shear. J of Basic Eng, 85 (1963) 519-527.
[13] M.L. Williams, On the stress distribution at the base of a stationary crack. ASME J. Appl. Mech, 24(1957) 109-114.
[14] Q.Z. Xiao, B.L. Karihaloo, Coefficients of the crack tip asymptotic field for a standard compact tension specimen. Int J Fract, 118(1) (2002) 1-15.
[15] M. Grédiac, F. Hild Mesures de champs et identification en mécanique des solides. Collection Mécanique et Ingénierie des matériaux. Ed. Lavoisier, 2011.
[16] VB Pham, H-A Bahr, U. Bahr and H. Balke and H-J Weiss. Global bifurcation criterion for oscillatory crack path instability. Physical Review E (Statistical, Nonlinear, and Soft Matter Physics). 77 (2008), 66-114.